2009

Electronic and Structural Properties of Molybdenum Thin Films as Determined by Real Time Spectroscopic Ellipsometry

J. D. Walker

H. Khatri

V. Ranjan

Jian Li

R. W. Collins

See next page for additional authors

Original Publication Citation

Walker, J.D., Khatri, H., Ranjan, V., Li, J., Collins, R.W., & Marsillac, S. (2009). Electronic and structural properties of molybdenum thin films as determined by real-time spectroscopic ellipsometry. *Applied Physics Letters, 94*(141908), 1-3. doi: 10.1063/1.3117222

AIP | Applied Physics Letters

Electronic and structural properties of molybdenum thin films as determined by real-time spectroscopic ellipsometry

J. D. Walker, H. Khatri, V. Ranjan, Jian Li, R. W. Collins, and S. Marsillac

Citation: Applied Physics Letters **94**, 141908 (2009); doi: 10.1063/1.3117222
View online: http://dx.doi.org/10.1063/1.3117222
View Table of Contents: http://scitation.aip.org/content/aip/journal/apl/94/14?ver=pdfcov
Published by the AIP Publishing

Electronic and structural properties of molybdenum thin films as determined by real-time spectroscopic ellipsometry

J. D. Walker, H. Khatri, V. Ranjan, Jian Li, R. W. Collins, and S. Marsillac[a)]
Center for Photovoltaics Innovation and Commercialization (PVIC), University of Toledo, Toledo, Ohio 43606, USA

(Received 17 March 2009; accepted 19 March 2009; published online 8 April 2009)

Real-time spectroscopic ellipsometry (RTSE) is shown to be an effective contactless probe of radio frequency magnetron sputtered molybdenum thin films used as the back electrode in chalcopyrite $[Cu(In,Ga)Se_2]$ solar cells. A series of Mo thin films was sputtered onto soda-lime glass substrates at Ar pressures ranging from 4 to 20 mTorr. RTSE measurements reveal how Ar pressure affects the nucleation and growth mechanisms that influence the films' ultimate grain structure and properties. Determinations of the free electron relaxation times at optical frequencies reveal that higher pressures lead to a smaller average grain size and increased void volume fraction. © *2009 American Institute of Physics*. [DOI: 10.1063/1.3117222]

Molybdenum thin films are utilized widely as the back electrode in copper indium-gallium diselenide $[Cu(In,Ga)Se_2]$ thin-film solar cells—this being one of the most promising of the thin-film photovoltaics technologies.[1] In this study we investigate the use of *in situ* and *ex situ* characterization techniques for sputtered Mo thin films, and in particular, are interested in monitoring and controlling the deposition process. The ability to extract quantitative information in real time by real-time spectroscopic ellipsometry (RTSE) is anticipated to be important in evaluating the $Cu(In,Ga)Se_2$ solar cell fabrication process.

Molybdenum thin films were deposited by rf magnetron sputtering onto soda-lime glass substrates at room temperature using a high purity (99.95%), 2 in. diameter Mo target in high purity (99.998%) argon. A 10 SCCM (SCCM denotes cubic centimeter per minute at STP) Ar flow rate was used and the pressure was varied from 4 to 20 mTorr by adjusting the Ar pumping rate. The rf power was set at 100 W for all depositions. RTSE data were acquired *in situ* during film growth using a rotating-compensator multichannel ellipsometer with a photon energy range of 0.75–6.5 eV at an angle of incidence of 65°. Pairs of (ψ,Δ) spectra were collected with an acquisition time of 1.5 s. Analyses of the spectra involved numerical inversion and least-squares regression algorithms. The optical model for the film consisted of a bulk layer whose dielectric function is determined in the analysis and a surface roughness layer whose dielectric function is determined from an effective medium theory as a 0.5/0.5 volume fraction mixture of bulk layer material and void.[2] Complementary *ex situ* characterization of the as-deposited film included x-ray diffraction (XRD), atomic force microscopy (AFM), and resistivity by four-point probe measurements.

RTSE is useful in studying the growth kinetics of thin films. Figure 1 shows the time evolution of the surface roughness and bulk layer thicknesses for Mo thin films deposited at three representative pressures as extracted in the same analyses that provide the time evolution of the dielectric function. Two distinct bulk layer growth rate regimes are visible for each deposition. The first is associated with thin film nucleation on the substrate surface. The second is associated with the fully coalesced film and has been applied in linear extrapolations to deduce thicknesses >60–100 nm, above which the film is opaque. The extrapolated final film thicknesses from RTSE agree well (to within 15%) with those obtained by profilometry. The decrease in deposition rates with increasing pressure in both regimes is due to increased scattering of the incident sputtered Mo atoms by the increasingly dense Ar ambient.

At time zero in Fig. 1, the shutter of the sputter gun is opened to initiate deposition. Immediately thereafter, the incident Mo atoms nucleate in the form of islands, a process evidenced by an abrupt increase in the surface roughness layer thickness.[3] A subsequent abrupt decrease in surface roughness can be attributed to the coalescence of these islands. After complete coalescence and during bulk layer growth, a further increase is observed in the surface roughness thickness, which gradually saturates to a stable value that increases with increasing pressures. A closer comparison of the results of Fig. 1 indicates that at the lowest pressure, bulk layer growth occurs simultaneously with island growth and coalescence, whereas at the highest pressure, bulk layer

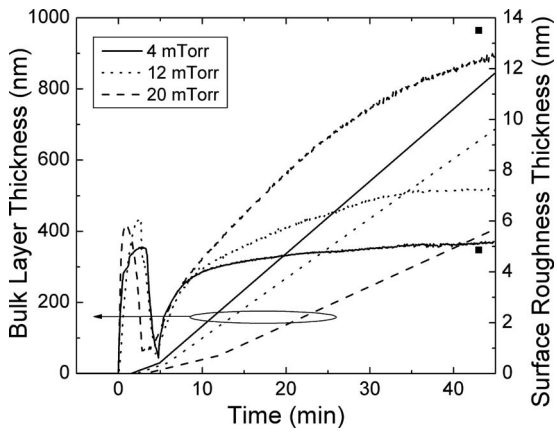

FIG. 1. Surface roughness and bulk layer thicknesses vs deposition time obtained by RTSE (lines) for Mo depositions at three Ar pressures. Also shown are scaled AFM rms roughness values for the final films at the extremes in pressure (points).

a)Electronic mail: sylvain.marsillac@utoledo.edu.

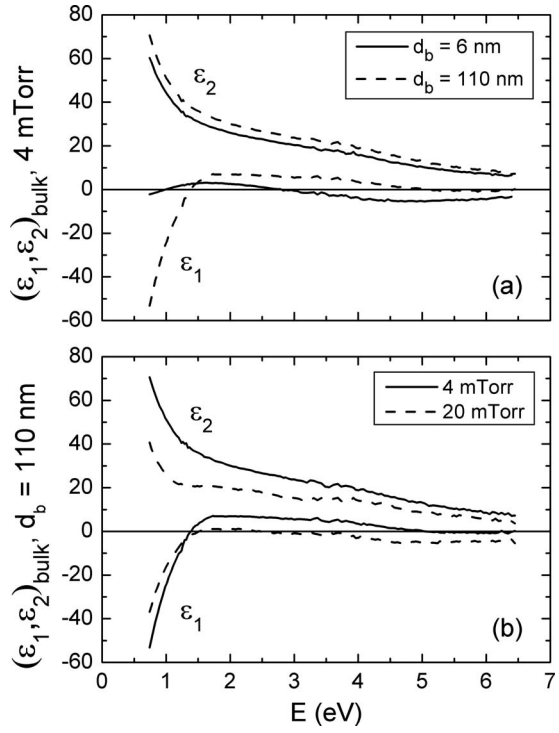

FIG. 2. Bulk layer dielectric functions $\varepsilon=\varepsilon_1+i\varepsilon_2$ of (a) one Mo film at two representative bulk layer thicknesses (d_b) at an Ar pressure of 4 mTorr and (b) two Mo films deposited at different Ar pressures at a fixed d_b value of 110 nm.

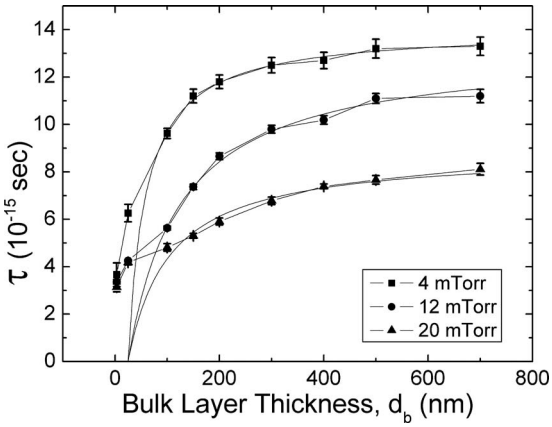

FIG. 3. Free electron relaxation time plotted as a function of bulk layer thickness for Mo films deposited at three different deposition pressures. Also shown are the results of fits using a simple conical grain growth model.

growth occurs only after complete island coalescence has occurred. This difference is believed to reflect the near-interface densification at low pressures due to enhanced ion bombardment that also leads to a lower void volume fraction in the final bulk film.

The observation in Fig. 1 that higher Ar pressures lead to rougher surfaces is corroborated by AFM images of surface topography. The average root mean square (rms) surface roughness thickness d_{AFM} from tapping mode AFM (5×5 μm^2 area) ranged from 3.6 to 10 nm with the increase in Ar pressure from 4 to 20 mTorr. These results agree well with the final RTSE surface roughness thicknesses d_s of Fig. 1, ranging from 5 to 13 nm, implying a relationship between the RTSE and AFM roughness values of $d_s \sim 1.35 d_{\mathrm{AFM}}$. This relationship is close to that obtained for silicon thin films.[4] The average rms roughness values from AFM, scaled according to this relationship, are indicated in Fig. 1 for the pressure extremes.

Because a single layer model was assumed for the bulk Mo layer in order to deduce the real and imaginary parts of its dielectric function, the effects of structural and optical property gradients within the films must be considered. The relatively short penetration depth of the light in Mo, namely, 16 nm at 0.75 eV and 11 nm at 3.0 eV (as determined from the ~800 nm bulk layer of the 4 mTorr film), implies that measurements of the dielectric function and its thickness evolution derive from this near-surface region of the film and as such represent an average property. The consistency of the correlations reported in this study suggests that this average property is meaningful. Such dielectric functions are compared in Fig. 2(a) at thicknesses of 6 and 110 nm for the film deposited with an Ar pressure of 4 mTorr and in Fig. 2(b), at a thickness of 110 nm for the films deposited with the Ar pressure extremes of 4 and 20 mTorr. Two effects can be noted by inspection of Fig. 2.

First for a given deposition pressure, as shown by the example of Fig. 2(a), the much larger decrease in ε_1 with decreasing photon energy below 1.5 eV for thicker films is attributed to a much longer intraband relaxation time compared to that of thinner films.[3] This in turn suggests a larger grain size and, thus, reduced grain boundary scattering in the thicker film. A similar effect on the decrease in ε_1, but weaker, occurs in Fig. 2(b) with decreasing pressure, indicating a longer relaxation time and larger grain size in the film deposited at lower pressure. This latter effect was corroborated by application of the standard Scherrer formula to the full width at half maximum of the (110) XRD peak measured for the Mo films after deposition at the different pressures.

Second, for a given thickness as shown in Fig. 2(b), the higher amplitude of ε_2 at high photon energies for the film deposited at lower pressure is attributed to stronger optical absorption associated with the interband transitions compared to that of the high pressure film. This in turn suggests a lower void volume fraction in the bulk of the film deposited at lower pressure. A similar increase in the amplitude of ε_2, but weaker, occurs in Fig. 2(a) with increasing thickness, indicating densification as the film grows. The former effect of deposition pressure has been corroborated through XRD measurements of the films, which showed an increase in the intensity of the (110) peak with decreasing pressure, indicating an increase in the packing density of crystallites in the films.

In order to explore the variations of Fig. 2 quantitatively, intraband electronic relaxation times at optical frequencies were extracted from the RTSE data sets collected during film growth at each pressure. This was done by fitting the dielectric functions over the low energy range (0.75–3.0 eV) to an analytical expression with Drude and Lorentz oscillator terms.[5] Overall, the parameter of greatest interest is the Drude energy broadening Γ, which is inversely proportional to the intraband electron relaxation time τ at optical frequencies, i.e., $\tau=h/\Gamma$, where h is Planck's constant.[5] The intraband relaxation time is plotted as a function of bulk layer thickness in Fig. 3 for the Mo films at the three representative deposition pressures.

In the Drude theory of metals, the dc resistivity is inversely proportional to the relaxation time τ as measured

optically, based on the assumption that the same scattering mechanism holds for electrons in response to dc and optical fields.[5] In fact, the resistivity of the films as determined by four-point probe in conjunction with film thickness measurements correlate well with the inverse of the relaxation time from Fig. 3 at the end of the deposition. The RTSE-deduced τ values and the four-point probe resistivity results both can be understood through a reduction in grain size with increasing pressure, as verified by XRD. In addition, the increase in void volume fraction in the Mo films with increasing deposition pressure may also contribute to the shorter relaxation time and higher resistivity.

The dependence of the electronic relaxation time on bulk layer thickness in Fig. 3 can be understood using a simple model of grain boundary scattering as proposed by Kasap[6] and Mayadas *et al.*,[7]

$$\tau^{-1} = \tau_b^{-1} + \frac{3v_F\Re}{2\lambda_g(1-\Re)}. \quad (1)$$

In Eq. (1), τ_b is the relaxation time in the limit of infinite grain size, $v_F = 1.7 \times 10^6$ m/s is the Fermi velocity for Mo, λ_g is the electron mean free path, and $\Re$ is the grain boundary reflection coefficient, taken to be 0.5 as the first approximation.[8] Excellent fits to the data for τ in Fig. 3 with bulk layer thicknesses greater than 25 nm (solid lines) are obtained if one assumes that the mean free path λ_g is equal to the grain radius and that the crystallite evolution follows a conical growth mode in accordance the relationship $\lambda_g = (d_b - d_o)\tan\theta$, where θ is the half-angle of the conical crystallites. Fitting for θ and calculating the average final film grain radius λ_g reveals a clear trend of decreasing grain size with increasing deposition pressure consistent with the XRD results. The existence of a cone growth offset of $d_o \sim 25$ nm and a saturation in $\tau \sim 3.5 \times 10^{-15}$ s below the same thickness is an indication that the grain size does not decrease continuously with decreasing thickness, but rather saturates at sizes on the order of 10 nm.

In conclusion, Mo thin films were grown by rf magnetron sputtering and characterized by *in situ* RTSE and *ex situ* AFM, XRD, and resistivity. Real-time growth mechanisms are shown to be accessible through RTSE. Two major structural effects were observed and discussed. First, RTSE dielectric functions were modeled using a Drude term with a variable electronic relaxation time τ. The noncontacting RTSE results were consistent with resistivity measurements and revealed a structural trend of decreasing grain size with increasing deposition pressure. This trend was corroborated by a measure of the grain size based on the XRD peak width. Second, the incorporation of greater structural heterogeneity including thicker surface roughness layers and higher void volume fractions in the bulk layer were observed with increasing deposition pressure in the range of 4–20 mTorr. These results were corroborated by AFM images and by a decreasing (110) XRD peak intensity, respectively.

This work was supported by AFRL Contract No. FA9453-08-C-0172, Vehicles Directorate, Kirtland AFB.

[1] I. Repins, M. A. Contreras, B. Egaas, C. DeHart, J. Scharf, C. L. Perkins, B. To, and R. Noufi, Prog. Photovoltaics **16**, 235 (2008).
[2] H. V. Nguyen, I. An, and R. W. Collins, Phys. Rev. B **47**, 3947 (1993).
[3] I. An, H. V. Nguyen, N. V. Nguyen, and R. W. Collins, Phys. Rev. B **65**, 2274 (1990).
[4] J. Koh, Y. Lu, C. R. Wronski, Y. Kuang, R. W. Collins, T. T. Tsong, and Y. E. Strausser, Appl. Phys. Lett. **69**, 1297 (1996).
[5] R. W. Collins and A. S. Ferlauto, in *Handbook of Ellipsometry*, edited by H. G. Tompkins and E. A. Irene (William Andrew, Norwich, NY, 2005), Chap. 2.
[6] S. O. Kasap, in *Principles of Electronic Materials and Devices*, 3rd ed. (McGraw-Hill, New York, 2006), pp. 168–170.
[7] A. F. Mayadas, M. Shatzkes, and J. F. Janak, Appl. Phys. Lett. **14**, 345 (1969).
[8] S. Marsillac, N. Barreau, H. Khatri, J. Li, D. Sainju, A. Parikh, N. J. Podraza, and R. W. Collins, Phys. Status Solidi C **5**, 1244 (2008).